NOTES AND CORRESPONDENCE

Skewness of Spatial Gradients of Turbulent Dissipation Rates in the Mixed Layer

S. A. THORPE

School of Ocean Sciences, Menai Bridge, Anglesey, United Kingdom

T. R. OSBORN

Department of Earth and Planetary Sciences, The Johns Hopkins University, Baltimore, Maryland

(Manuscript submitted 4 June 2004, in final form 3 January 2005)

ABSTRACT

Temperature ramps or microfronts are coherent tilted structures in the oceanic and atmospheric boundary layers at which there are small, but detectable, changes in mean temperature. Their presence contributes to a nonzero skewness, $S_T(\theta)$, of the spatial derivatives of temperature, dT/dx, at constant depth within the ocean mixed layer. The skewness $S_T(\theta)$ has a roughly sinusoidal variation with θ, the direction in which the derivatives are measured relative to the wind. The magnitude of the skewness, $|S_T(0)|$, measured in a direction into the wind ($\theta = 0$) is of order unity, and the sign of $S_T(0)$ depends on the heat flux from the air to the water through the sea surface, being positive if the heat flux is positive. Recent observations using an AUV, Autosub, have shown that the mean values of ε, the rate of dissipation of turbulent kinetic energy per unit mass, change as temperature ramps are crossed. This observation raises the questions: Is the skewness of the gradient of $\log\varepsilon$, $S_{\log\varepsilon}(\theta)$, nonzero in the mixed layer even though ε is observed to be lognormal? If so, is $S_{\log\varepsilon}(\theta)$ related to $S_T(\theta)$? The answer to both of the questions appears to be "yes," although the magnitude of $S_{\log\varepsilon}(\theta)$ is small, of order 5×10^{-2}, and no clearly detectable variation with θ is found in the available data.

1. Introduction

a. Temperature ramps or microfronts

The existence of coherent structures in stratified turbulent boundary layers, now referred to as temperature ramps or "microfronts," has been known for some time. They are found in the boundary layers of the atmosphere, the ocean, and lakes (see, e.g., Screenivasan and Antonia 1977; Antonia et al. 1979; Thorpe and Hall 1980; Thorpe 1985; Thorpe et al. 1991). They consist of thin regions of high temperature gradient advected by the mean flow and tilted forward in the downwind direction at some 45°–60° from the horizontal. In the upper mixing layers of the ocean and lakes, the ramps are structures with temperature changes of typically 5–10 mK over horizontal distances of 0.05–0.2 m, coherent over vertical scales of a few meters and often at least a quarter of the mixed layer depth, and their separation is typically 1.5 times the layer depth. They divide regions of relatively high and low bubble populations (Thorpe and Hall 1987), suggesting an association with advective motions that carry bubbles from their source in breaking waves downward into the mixed layer. The ramps are also known to be locations of abrupt changes in current speed (Thorpe and Hall 1980). They appear to be associated with large eddies modified by, and possible resulting from, the shear in the mixed layer.

b. Skewness

The presence of temperature ramps contributes to a skewness S_T in the gradient of temperature when measurements are made by sensors moving horizontally along legs (tracks in fixed directions at constant depth) made through the water at speeds exceeding the mean flow (or, for measurements at a fixed location, to a skewness in the time derivative of temperature). Skewness S_T is of order unity and its sign depends on that of the surface heat flux and on the direction θ of legs

Corresponding author address: Dr. Steve A. Thorpe, Bodfryn, Glanrafon, Llangoed, Anglesey, LL58 8PH, United Kingdom.
E-mail: oss413@sos.bangor.ac.uk

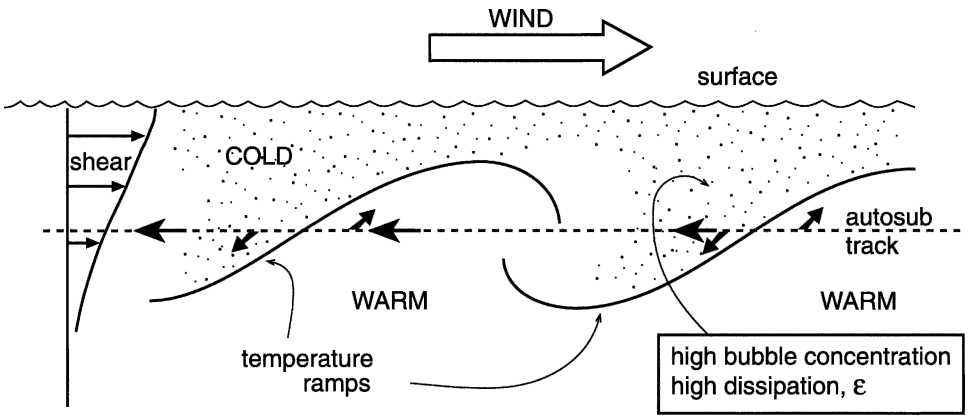

FIG. 1. Sketch of the two-dimensional structure of a temperature ramp in the surface-cooling conditions of the observations. Bubbles found on the colder side of the ramps lead to enhanced acoustic scatter. The dashed line shows the right-to-left track of the Autosub AUV when $\theta = 0°$. The shape or structure of the ramps in the third dimension, that normal to the plane shown here, is presently unknown. (Adapted from Thorpe et al. 2003a.)

relative to the wind. For legs made upwind ($\theta = 0°$) at speeds faster than the mean flow, S_T is generally positive in conditions of surface heating and negative for cooling conditions, with the reverse for downwind legs. Data described below were obtained using an AUV, Autosub. The presence of ramps sketched in Fig. 1 encountered along the horizontal, right-to-left track of the AUV, lead to abrupt falls in the measured temperature as the AUV moves across a ramp into colder water, contributing to a negative skewness of temperature gradient. The sign of S_T is reversed for legs in reciprocal directions, but the magnitude remains unchanged. Small, but nonzero, values of S_T are found for across-wind tows ($\theta = \pm 90°$), consistent with a turning of the flow in sense consistent with an Ekman flow (Thorpe 1985; Soloviev 1990; Thorpe et al. 1991; Wijesekera et al. 2004).

c. Generation of ramps

The nature of the motions associated with ramps, and consequently their effect in generating or advecting turbulence, is not entirely clear. It appears possible that the ramps are braids within large Kelvin–Helmholtz billows developing in the near-critical flow of a weakly, stably stratified mixed layer (as suggested by the stability analysis of Thorpe and Hall 1977), that in convective conditions they are associated with the formation of convective plumes, or that they may have structures and origins similar to those of "bursts" or horseshoe (or hairpin) eddies that occur in flow over solid boundaries (see, e.g., Gerz and Schumann 1996), perhaps initiated or augmented by the rotational motions (e.g., rotors; Melville et al. 2002) produced by breaking waves. No evidence has been found that below the Langmuir circulation convergence regions, commonly marked on the water surface by windrows, ramps are more or less common than elsewhere in spite of the expectation that the downwind flow, and cross-wind component of vorticity, may be greater in such regions (Thorpe 2004), favoring shear instability with billow and braid formation. Any connection between the two phenomena, temperature ramps and Langmuir circulation, is yet to be established (Thorpe et al. 2003a).

d. The observations

Thorpe et al. (2003a) describe how the AUV, Autosub, was instrumented and used to make measurements, including those of turbulent dissipation rates ε and temperature along 5-km legs at constant depths and directions in the surface mixed layer of the Atlantic off the west coast of Scotland in conditions of weak, but unquantified, surface cooling. Each leg took about one hour to complete. A turbulence package mounted on the nose of the AUV supported airfoil probes for velocity microstructure and a Thermometrics FP07 thermistor to determine temperature gradient. Frequency response was not measured for our specific sensor but reports on the same, widely used, model by Vachon and Lueck (1984) and Gregg (1999) suggest that the spectral, half-power point is in the neighborhood of 25 Hz at the AUV speed of about 1.25 m s^{-1} and imply that the sampling will provide adequate resolution of the gradients used as described below to determine S_T. Bubble concentrations are determined using sidescan sonar and a bubble resonator (Farmer et al. 1998) carried on the AUV and are described by Thorpe et al. (2003a,b).

The observations show that the rates of dissipation of turbulent kinetic energy per unit mass, ε, measured along horizontal AUV tracks in the mixed layer are consistent with the law of the wall at depths of (1.55–15.9)H_s, where H_s is the significant wave height, and have pdfs close to lognormal. Conditional sampling, in which data are selected and averaged together around the times of the detection of temperature ramps, shows that on average the ramps have an associated horizontal gradient in the mean ε with relatively higher dissipation rates on the side of the front enriched in bubbles and consequently of higher void fraction, as illustrated in Fig. 1. The pattern appears to be a consequence of the downward advection of the higher levels of turbulence (and of bubbles) from near the surface by the coherent motions leading to the ramps. Vertical displacements of the mean AUV depth of order 2–6 cm over some 10-m horizontal scale are found near the ramps, upward on the cold side and downward on the warm, consistent with the postulated vertical motion (Thorpe et al. 2003a). The displacements appear too small to produce any substantial bias in the observed temperatures or significant distortion of the observed ramp structure.

The related changes in temperature and ε as temperature ramps are crossed suggest that the skewness of the spatial gradient of ε, like that of temperature, may be nonzero in the turbulent upper ocean mixed layer. The changes encountered as the AUV advances along the track, illustrated in Fig. 1, abrupt decreases in mean temperature and increases in ε, imply that the corresponding skewness gradient values should be of opposite signs and that the magnitudes of the two skewness values may possibly be related. Because of the intermittency of ε and its high attendant positive skewness (typically 3–5) and large kurtosis (typically 20–45), skewness values of sequential differences, proportional to the gradient of ε, tend to be very variable, and estimates made along the Autosub legs, even though derived from some 3600 1-s sequential estimates of ε, are less robust than those of the normally distributed logε. It was therefore decided to focus attention on the skewness of logε rather than of ε.

The purpose of this note is therefore to report on measurements of the skewness of the horizontal gradients of logε, a hitherto unquantified statistical measure of variation in the mixed layer, and examine its relation to the skewness of temperature gradients. This provides further evidence of the dynamical role played by the coherent structures in the mixed layer of which temperature ramps are one example.

The AUV, Autosub, moves through the water at an almost constant speed of 1.25 m s^{-1}, and temporal derivatives translate immediately into spatial ($d/dt = ud/dx$) provided the Taylor frozen field approximation is valid. In the analysis carried out below, temperature gradient is calculated from the differences of 0.5-s averaged temperatures or over horizontal distances of 0.63 m. Dissipation rates are estimated every 1.0 s, corresponding to horizontal distances of about 1.25 m, and these are used to determine the dissipation gradients. Skewness values are estimated along separate 5-km legs. Data are derived from observations at 1.6–10.5-m depth in a mixed layer at least 12 m thick and in winds ranging from 4–13 m s^{-1} but mostly in the higher end of the range, conditions further described in Thorpe et al. (2003a).[1]

2. Results

a. Skewness of temperature gradients

Figure 2 shows the skewness of temperature derivatives, $S_T(\theta)$, as a function of θ, the angle between the direction of the AUV track and the wind direction. (A track directly into wind has $\theta = 0$; see inset to figure.) The skewness has a roughly sinusoidal variation with θ, but there is considerable scatter. The skewness near $\theta = 0$ is negative, consistent with a cooling of the water surface during the period of observations. The scatter of values obtained in legs made in similar wind speeds, depth, and inclination to the wind direction θ suggests an uncertainty in the estimates of $S_T(\theta)$ of about ± 0.25 (shown by the error bar) or a contribution of this magnitude caused by undetermined processes. This uncertainty is consistent with the scatter found in earlier estimates of $S_T(\theta)$, for example, by Thorpe (1985) and by Wijesekera et al. (2004, their Fig. 3a). Some unaccounted-for variability in skewness may, for example, be caused by variations in wind direction and speed (i.e., gustiness). The uncertainty of estimates of the mean wind direction during legs is about $\pm 10°$.

The effect of varying the averaging time and time interval between records from which gradients are estimated from values of 0.25–4 s and covering the 1-s periods of the dissipation estimates produces no significant variation in $S_T(\theta)$.

b. Skewness of turbulent dissipation

Figure 3 shows $S_{\log\varepsilon}(\theta)$ plotted against $S_T(\theta)$ for the same legs and therefore for the same values of θ. The turbulence dissipation skewness $S_{\log\varepsilon}(\theta)$ lies between

[1] The data analyzed come from the mission legs 1.1–1.16, 2.1–2.15, and 4.23–4.28 described in Thorpe et al. (2003a).

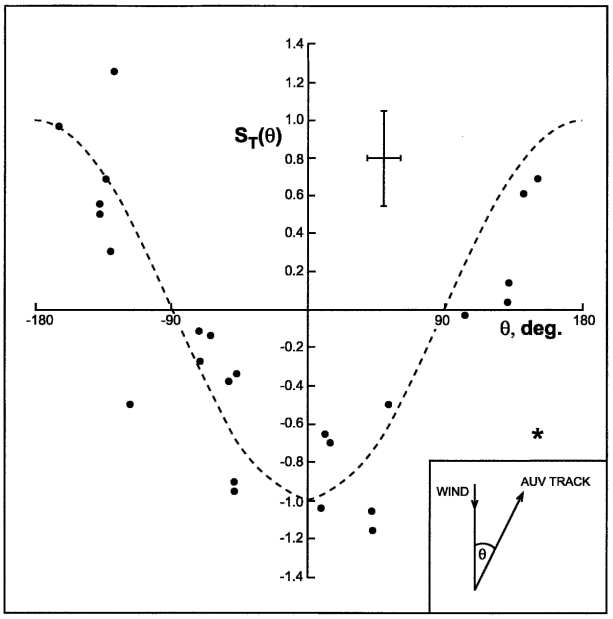

FIG. 2. The variation of the skewness of the temperature time derivative $S_T(\theta)$ as a function of θ. The dashed curve shows the sinusoidal curve, $S_T(\theta) = -\cos\theta$, with unit amplitude. A definition sketch for θ is shown. The point marked with a star refers to a leg made during a falling wind and with the lowest mean wind speed, 4 m s^{-1}, of the dataset. Error bars show the uncertainty of the observations. That in the wind direction represents the uncertainty of 10° in its determination. The range of uncertainty in skewness is determined from the mean differences between the absolute values of skewness estimated in sequential pairs of legs that are made at the same depth and at approximately equal angles to the wind so as to minimize the unknown effects of different winds or depths.

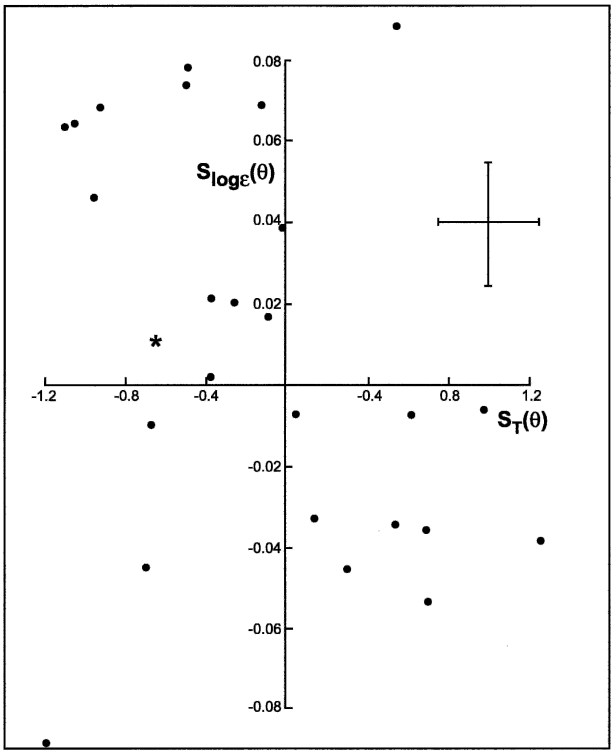

FIG. 3. The variation of the skewness of the time derivative of logε, $S_{\log\varepsilon}(\theta)$, with the skewness of the temperature time derivative $S_T(\theta)$. The point marked with a star corresponds to that in Fig. 2. Error bars show the ranges of uncertainty in the values of skewness determined as in Fig. 2.

-0.084 and $+0.088$ with a mean value of the modulus, $|S_{\log\varepsilon}(\theta)|$, equal to 0.041.[2] The points are scattered, but the majority (22 of the 26 estimated values) lie in the second and fourth quadrants, suggesting a negative proportionality between the two sets of skewness estimates. The mean ratio, $R = S_{\log\varepsilon}(\theta)/S_T(\theta)$, is equal to –0.222, but with a standard deviation of 0.744 largely resulting from a single value of R that is inflated by a very low value of $S_T(\theta)$ and without which the mean R is equal to -0.075 with a standard deviation of 0.119. The correlation coefficient of the two sets of skewness values is -0.37. This is significant at the 10% level. There appears to be nothing exceptional about the four points that lie in the first and third quadrants of the figure: they are from legs spanning the depth range of 3.6–10.4 m but all are in winds of 10–12 m s^{-1}.

Unlike $S_T(\theta)$, there is no evidence that $S_{\log\varepsilon}(\theta)$ may have a simple sinusoidal (or other direct) variation with θ, even when data are constrained to those collected in a single 24-h period in which the wind was fairly steady, averaging 11.4 m s^{-1}.

No significant variation in $|S_T(\theta)|$ or in $|S_{\log\varepsilon}(\theta)|$ is found with depth. There is an indication that the mean $|S_{\log\varepsilon}(\theta)|$ estimates increase in magnitude as the averaging and differencing time interval is increased from 1 s to 2 s and 4 s, but mean values still lie within the uncertainty of the 1-s estimates.

3. Discussion

Since only 4 of the 26 points of Fig. 3 lie in the quadrants in which R is positive, there does appear to be a significant probability that there is a relationship between the signs of the two skewness values; the probability of fewer than 5 successes in 26 attempts if the chance of success and failure are equal is 2.67×10^{-4}. The majority of skewness gradient values of temperature and logε are therefore of opposite sign, in accordance with the expectation expressed in section 1d and based on the changes illustrated in Fig. 1. The order of magnitude of $S_{\log\varepsilon}(\theta)$ is, however, an order of magni-

[2] The values of the modulus of the skewness of the gradient of ε are of order unity.

tude less than that of $S_T(\theta)$, and $S_{\log\varepsilon}(\theta)$ is, at best, only very weakly correlated to $S_T(\theta)$, suggesting possible differences in the physical processes leading to the skewness of temperature and dissipation rate ε, that is, to the distribution of the two quantities in the mixed layer. One such difference in processes may be the generation of turbulence in the shear zone at the temperature ramps for which there is evidence, although weak, in the conditional sampling described by Thorpe et al. (2003a), but this can only be resolved by measurements of ε (accompanied by temperature) with improved spatial resolution, preferably to scales of order 0.1 m, a demanding requirement.

It is likely that the skewness $S_{\log\varepsilon}(\theta)$ is nonzero in other boundary layers, but estimates have yet to be made. The authors know of no estimates of temperature gradient skewness in the bottom or benthic boundary layer over level topography, but measurements from moored instruments on continental slopes show negative skewness of the time derivative of temperature, consistent with a sudden arrival of upslope-moving colder water in the "internal swath zone" affected by incident internal waves (Thorpe et al. 1991), with values of skewness that are in accord with those found in a numerical model by Legg and Adcroft (2003).

More information is required of the temperature ramps to establish their nature and cause, or causes. Observations are needed to establish the structure of the ramps and temperature field in the direction of the mean horizontal vorticity vector in the mixed layer (or a horizontal direction normal to the wind). The only information at present about the three-dimensional structure of ramps seems to be limited to four examples described by Thorpe and Hall (1980, see their Fig. 5) and obtained using a moored three-dimensional array of thermistors in a large lake. Coherent structures with high temperature gradients persist in the spanwise direction for some 3 m at 6.55-m depth when the ramps were coherent from depths from 4.55 to 7.05 m. The data are insufficient and too limited in their lateral extent to draw any definite conclusions about ramp structure or cause, and the related velocity fluctuations and pattern of turbulent dissipation are unknown. More generally, the vortical structure within the mixed layer and its relation to turbulent dissipation rates deserve further investigation if the processes within the mixed layer are to be properly understood.

In view of the variation in water properties suggested in Fig. 1 and quantified by Thorpe et al. (2003a), it is likely that, in addition to the gradients of temperature and the rate of dissipation of turbulent kinetic energy ε, the skewness of the horizontal gradients of bubble void fraction and of the (related) acoustic scattering cross section will generally be nonzero within the surface mixed layer of the ocean and lakes.

Acknowledgments. Part of this research was undertaken with funding from NERC Grant NER/A/S/2000/00359. TRO was supported by the Office of Naval Research (Grant N000149910088). We thank Kate Davis for assistance in the preparation of figures.

REFERENCES

Antonia, R. A., A. J. Chambers, C. A. Friehe, and C. W. Van Atta, 1979: Temperature ramps in the atmospheric surface layer. *J. Atmos. Sci.,* **36,** 99–108.

Farmer, D. M., S. Vagle, and A. D. Booth, 1998: A free-flooding acoustical resonator for measurements of bubble size distributions. *J. Atmos. Oceanic Technol.,* **15,** 1132–1146.

Gerz, T., and U. Schumann, 1996: A possible explanation of countergradient fluxes in homogeneous turbulence. *Theor. Comput. Fluid Dyn.,* **8,** 169–181.

Gregg, M. C., 1999: Uncertainties and limitations in measuring ε and χ_T. *J. Atmos. Oceanic Technol.,* **16,** 1483–1490.

Legg, S., and A. Adcroft, 2003: Internal wave breaking at concave and convex continental slopes. *J. Phys. Oceanogr.,* **33,** 2224–2246.

Melville, W. K., F. Veron, and C. J. White, 2002: The velocity field under breaking waves: Coherent structures and turbulence. *J. Fluid Mech.,* **454,** 203–234.

Screenivasan, K. R., and R. A. Antonia, 1977: Skewness of temperature derivatives in turbulent shear flows. *Phys. Fluids,* **20,** 1986–1988.

Soloviev, A. V., 1990: Coherent structures in the ocean surface in convectively unstable conditions. *Nature,* **346,** 157–160.

Thorpe, S. A., 1985: Small-scale processes in the upper ocean boundary layer. *Nature,* **318,** 519–522.

——, 2004: Langmuir circulation. *Annu. Rev. Fluid Mech.,* **36,** 55–79.

——, and A. J. Hall, 1977: Mixing in upper layer of a lake during heating cycle. *Nature,* **265,** 719–722.

——, and ——, 1980: The mixing layer of Loch Ness. *J. Fluid Mech.,* **101,** 687–703.

——, and ——, 1987: Bubble clouds and temperature anomalies in the upper ocean. *Nature,* **328,** 48–51.

——, M. Curé, and M. White, 1991: The skewness of temperature derivatives in oceanic boundary layers. *J. Phys. Oceanogr.,* **21,** 428–433.

——, T. R. Osborn, J. F. E. Jackson, A. J. Hall, and R. G. Lueck, 2003a: Measurements of turbulence in the upper-ocean mixing layer using Autosub. *J. Phys. Oceanogr.,* **33,** 122–145.

——, ——, D. M. Farmer, and S. Vagel, 2003b: Bubble clouds and Langmuir circulation: Observations and models. *J. Phys. Oceanogr.,* **33,** 2013–2031.

Vachon, P., and R. Lueck, 1984: A small combined temperature–conductivity probe. *STD Conference and Workshop*, Marine Technology Society, San Diego Section, and the MIT Oceanic Instrumentation Committee, 126–131.

Wijesekera, H.W., C.A. Paulson and E.D. Skyllingstad, 2004: Scaled temperature spectrum in the unstable oceanic surface layer. *J. Geophys. Res.*, **109,** C03015, doi:10.1029/2003JC002066.